MORTAR DATING USING AMS ^{14}C AND SEQUENTIAL DISSOLUTION: EXAMPLES FROM MEDIEVAL, NON-HYDRAULIC LIME MORTARS FROM THE ÅLAND ISLANDS, SW FINLAND

Alf Lindroos[1] • Jan Heinemeier[2] • Åsa Ringbom[3] • Mats Braskén[4] • Árny Sveinbjörnsdóttir[5]

ABSTRACT. Non-hydraulic mortars contain datable binder carbonate with a direct relation to the time when it was used in a building, but they also contain contaminants that disturb radiocarbon dating attempts. The most relevant contaminants either have a geological provenance and age or they can be related to delayed carbonate formation or devitrification and recrystallization of the mortar. We studied the mortars using cathodoluminescence (CL), mass spectrometry (MS), and accelerator mass spectrometry (AMS) in order to identify, characterize, and date different generations of carbonates. The parameters—dissolution rate, ^{13}C/^{12}C and ^{18}O/^{16}O ratios, and ^{14}C age—were measured or calculated from experiments where the mortars were dissolved in phosphoric acid and each successive CO_2 increment was collected, analyzed, and dated. Consequently, mortar dating comprises a CL characterization of the sample and a CO_2 evolution pressure curve, a ^{14}C age, and stable isotope profiles from at least 5 successive dissolution increments representing nearly total dissolution. The data is used for modeling the interfering effects of the different carbonates on the binder carbonate age. The models help us to interpret the ^{14}C age profiles and identify CO_2 increments that are as uncontaminated as possible. The dating method was implemented on medieval and younger mortars from churches in the Åland Archipelago between Finland and Sweden. The results are used to develop the method for a more general and international use.

INTRODUCTION

It has been known since the 1960s that it is possible to date old lime mortars using standard radiocarbon carbonate procedures (Labeyrie and Delibrias 1964; Stuiver and Smith 1965). However, the method is sensitive to contamination effects that are poorly understood and has therefore been used with great precaution and with varying success in archaeometry (e.g. Baxter and Walton 1970; Folk and Valastro 1976; Van Strydonck et al. 1983; Willaime et al. 1983). Some systematic studies of mortar hardening and dissolution versus chemical activity of stable isotopes have been published (Pachiaudi et al. 1986; Van Strydonck et al. 1986, 1989; Van Strydonck and Dupas 1991; Ambers 1987), but the link to carbonate mineralogy and stable isotope geochemistry has been weak. Accelerator mass spectrometry (AMS) ^{14}C dating analyses of mortars have been reported by our research group over the past 10 yr (Ringbom and Remmer 1995, 2000, 2005; Heinemeier et al. 1997; Hale et al. 2003; Ringbom et al. 2006). In these publications, we have presented dates from the Åland Islands, as well as classical and medieval Rome and 17th century America. Several hundred samples have been dated in 2 or sometimes 3 CO_2 fractions, and more recently in 5 fractions. The dating method with sample preparation and quality control is based on the guidelines proposed by Folk and Valastro (1976) in their decay counting studies, but the sample quality control and the preparation techniques have been further developed. Cathodoluminescence (CL) was introduced to the sample control, and sequential dissolution and AMS were introduced into the dating procedure. The interpretation of the AMS data from the sequential sample dissolutions has been described earlier (Hale et al. 2003; Ringbom et al. 2003), but the theoretical foundations for the method, based on stable isotope activity of carbon and oxygen, has only been published locally in a doctoral thesis (Lindroos 2005). In this article, we will describe the theoretical background for the interpretation of AMS ^{14}C data of mortar. Different carbonate phases commonly present in non-hydraulic mortars will be described in terms of CL characteristics, dissolution behavior in phosphoric acid hydrolysis, stable

[1] Åbo Akademi University, Finland, Dept. of Geology and Mineralogy. Corresponding author. Email: alindroo@abo.fi.
[2] University of Århus, Denmark, AMS Dating Centre.
[3] Åbo Akademi University, Finland, Dept. of Art History.
[4] Swedish Polytechnic, Vasa, Finland.
[5] University of Iceland, Science Institute.

isotope signatures, and chemical activity. Case studies of medieval and younger mortars from the Åland Islands in the northern Baltic Sea will be presented and interpreted in these terms. The samples from Åland have been of great importance in developing the dating method for a more general use.

MINERALOGY OF NON-HYDRAULIC MORTARS

All mortars have several soluble carbonate phases that produce carbon dioxide during acid hydrolysis and contribute to the ^{14}C age of the mortar. Generally, we have the following common phases:

- The dominant and most relevant carbonate phase for dating in non-hydraulic mortars is the calcitic binder. In an ideal case, this phase has a well-defined ^{14}C age of historical or archaeological interest. The ^{14}C age reflects the hardening of mortar according to the reaction below (Equation 1).

$$Ca(OH)^2 + CO_2 \rightarrow CaCO_3 + H_2O \qquad (1)$$

Slaked lime + atmospheric carbon dioxide = calcite + water

- The binder is, however, a complex system of calcites with different growth history, habitus, and trace element and isotope chemistry. The most important factor controlling calcite growth is pH, which evolves from super-alkaline towards neutral during the hardening of the mortar.
- Calcitic lime lumps are very common. They may form before the mortar is mixed with an aggregate and used. The lumps are homogenous white spots of varying size. They are soft and often they display a concentric structure with a fine-grained crust and a more coarse-grained interior. The interior may have recrystallizations.
- The slaked lime usually contains residues of incompletely burned limestone. These residues are not identical to the original unburned limestone, as the high temperatures have altered their habiti, dissolution rate, and to some extent even their stable isotope signature (Lindroos 2005 and references therein).
- Recrystallizations caused by percolating water in mortared constructions are common.
- Natural stable carbonate minerals are very likely to be incorporated into the mortar paste during the mixing of the lime with a geological aggregate or filler materials like sand and gravel. The readily soluble minerals calcite and aragonite are of relevance for dating purposes, while other carbonate minerals are either rare or poorly soluble in cold phosphoric acid, which is typically used for acid hydrolysis and gas evolution. Common constituents are limestone and marble grains and splinters and sandstone grains with a carbonate matrix.
- It is common to find charcoal and ashes in mortars. Ashes contain calcite and potassium hydroxide. The former contributes directly to the ^{14}C age, and the latter raises the pH and affects the mineral chemistry and the chemical activities of the stable isotopes.

IDENTIFICATION AND CHARACTERIZATION OF THE MORTAR CARBONATES

The interpretation of ^{14}C data from a mortar containing several soluble carbonate phases of different ages requires that the carbonates are identified and that their solubility is either known or can be determined or modeled from data collected during the dissolution procedure. The CO_2 pressure curve and the stable isotope ratios of carbon and oxygen in the dated CO_2 gas increments are the most useful parameters as they are directly linked to the $^{14}C/^{12}C$ ratio determined for dating. It is important to consider the following properties.

Habitus

The mortar carbonates are usually easy to identify using a petrographic microscope (e.g. Deer et al. 1992). However, all carbonates are usually calcite and commonly they are all fine-grained. In thin sections of mortar, some of the phases can be readily identified, for example, natural aggregate carbonates such as marbles, lime lumps, and unburned residues, but there are usually problems as well:

- The non-hydraulic mortars are often soft, and it may be difficult to prepare proper thin sections.
- The natural carbonates may be fine-grained and very similar to the binder carbonates.
- The binder carbonates are not discrete phases with well-defined habiti, but continuous series with respect to crystallinity, trace element and stable isotope ratios, and sometimes even ^{14}C age when voluminous constructions are considered (Sonninen et al. 1985).
- A thin section represents only a small part of the usually rather heterogeneous sample. Fractures and voids with efflorescent recrystallizations may or may not have been included.
- After the sample has been crushed, sieved, and homogenized for dating, it is even more difficult to distinguish between the different carbonate phases.

A very useful complement to petrographic microscopy is cathodoluminescence (CL). This method is especially sensitive when it comes to distinguishing between carbonate phases with slightly different crystallinity and trace element chemistry (e.g. Marshall 1988). It is possible to inspect mortar pieces directly or after preparation of cut and polished surfaces. Grain-size fractions can be pressed into pellets, or alternatively the grains can be spread over a glass backing. We have used the latter approach because it requires less material and does not deform or break soft grains. It is possible to assess how many contaminants are in the grain-size fractions by performing image analyses (IA) (see e.g. Figure 14 and text), but the results are at best only semi-quantitative due to many problems (e.g. variable luminescence, segmentation problems, etc.; Lindroos 2005). Below, we present some CL images of common calcite phases in non-hydraulic mortars (Figure 1).

The most important factor determining the color and intensity of the luminescence is the Mn^{2+}/Fe^{2+} ratio in the calcite (e.g. Habermann et al. 2000). The chemical activity of these ions is controlled by the decreasing pH in crystallizing mortars.

Solubility

^{14}C dating and the determination of δ^{13}C and δ^{18}O of carbonates are carried out by phosphoric acid hydrolysis of the carbonates in the samples. In mass spectrometry (MS), the measurement is done directly on CO_2, while the AMS dating is performed after reduction to graphite. In our laboratory, concentrated H_3PO_4 (85 wt%) is used. By assuming that the dissolution rate (volume dissolved per unit time) is proportional to the remaining grain surface area, the dissolution course of a single, homogenous carbonate grain-size fraction can be modeled according to Equation 2:

$$\ln(1-F) = -\Gamma t \qquad (2)$$

where F is the progress variable (the dissolved fraction of the grain volume) going from $0 \rightarrow 1$, Γ is the dissolution constant, and t is the dissolution time. The relationship implies that the decrease of the radius of a dissolving grain is a linear function of time. It is strictly valid for spherical grains of uniform size and homogenous chemistry. Experiments on narrow grain-size windows of homogeneous marble and limestone splinter have shown that the dissolution can be fairly well modeled with Equation 2 (Lindroos 2005). Usually, the dissolution starts with a rapid release of CO_2, but the reaction stabilizes within a few seconds and can thereafter be described with a constant Γ value. A prac-
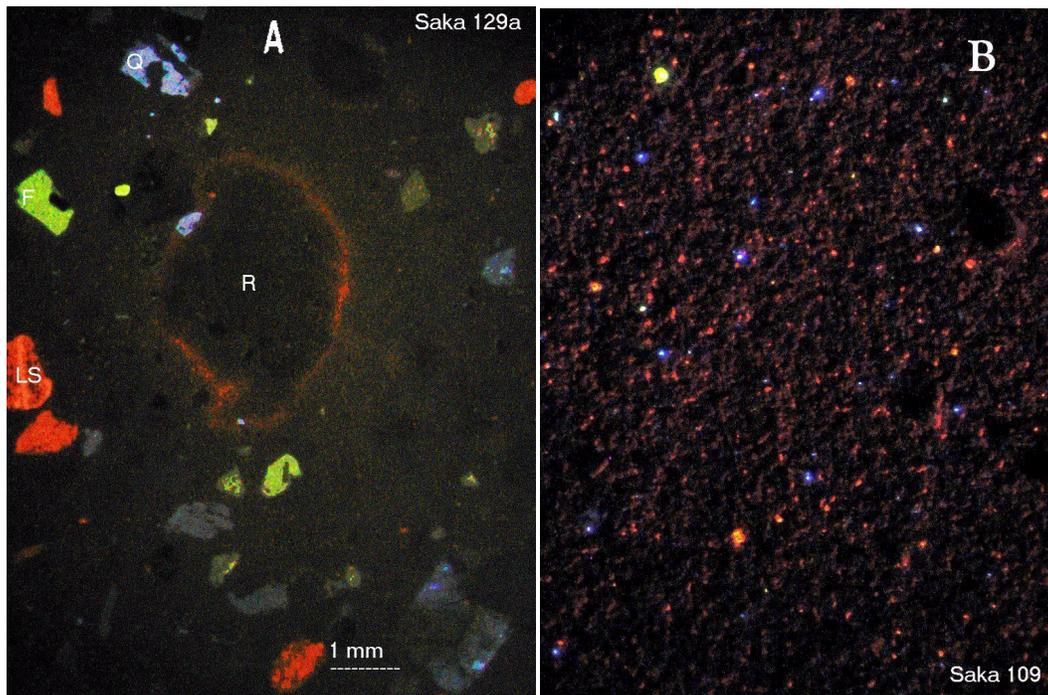
Figure 1 CL images of mortars from the church of Saltvik. A) Dark mortar binder with inclusions of limestone (LS) in red, quartz (Q) in blue, feldspar (F) in green, and a lime lump (R)—in this case a residue after lime burning. B) Grain-size fraction (<38 μm) from a contaminated sample.

tical problem to be considered is that very fine-grained fractions are sometimes used in dating because they are enriched in soft carbonates and the sample may originally have been small. This may cause modeling problems because the sample tends to float on the viscous acid, and no linear relation will be registered in the logarithmic plots.

Mortars are rarely single-carbonate systems, but instead tend to be multiphase systems with carbonates having different dissolution constants. They can be characterized in terms of discrete Γ values if the phases are significantly different, which is usually the case. Figure 2 shows a case where 3 carbonate phases having different dissolution constants add up to form a composite curve (Figure 2A). Time intervals dominated by CO_2 evolution from only 1 carbonate phase should define a straight line in the plot. Figure 2B presents the ^{14}C ages of the 4 increments and a final increment of the residue after overnight dissolution. The third increment represents 23.1% of the sample. Together with the second synchronous increment they represent 50.8% of the sample; their combined age of 736 ± 28 BP has been used in archaeometry (Ringbom and Remmer 2005 and references therein).

Isotopic Signature

Technical and natural carbonates usually differ significantly in their isotopic signatures. Therefore, it may be tempting to use the delta values (see Hoefs 2004) of carbon and oxygen isotopes as a measure of binder carbonates' contamination by limestone in the same way as in petrologic mixing systems. Mortar carbonate systems tend, however, to be too complex for similar modeling, and there are also some analytical problems to consider related to CO_2 solubility in the 85% acid (Walters et al. 1972; Wachter and Hayes 1985; Swart et al. 1991). Proper isotope measurements should be done
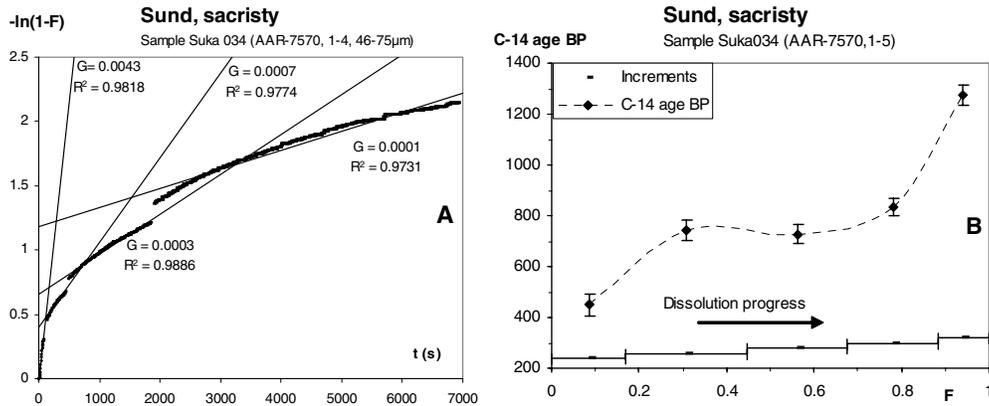
Figure 2 A) Cumulative CO_2 pressure curve converted to a $-\ln(1-F)$ versus t plot. For each increment, a Γ (G) value is defined and a regression line is fitted. The slopes of the lines are Γ values. The third increment has the best ln-linear fit, which is the most well-defined Γ value. The pressure drops during chill-outs of CO_2 have been omitted from the graph. B) ^{14}C ages and sizes of the increments 1–4 in A and a fifth increment from the residue.

using a large excess of dehydrated 100% acid; otherwise, the produced CO_2 will strive towards equilibrium with dissolved CO_2 in the water and acid and in the water produced during hydrolysis (Equation 1). This will lead to enrichment of heavy isotopes in solution and light isotopes in the gas phase. The equilibration process is, however, disturbed every time a gas increment is chilled out, but the general trend is towards a heavier isotopic signature towards the end of the dissolution. In our dissolution procedure, we usually extract the last increment after dissolution overnight. This increment is in near equilibrium with the dissolved phase that is enriched in heavy isotopes. Therefore, it tends to have a heavier signature regardless of whether it is affected by contaminants or not.

^{14}C Age

The hardening process of a mortar is relatively rapid compared with the half-life of ^{14}C and the resolution of the dating method. Normally, the hardening is completed within weeks or months at the surface of the mortar (Pachiaudi et al. 1986), but it can take years and decades before the whole construction has carbonated (Delibrias and Labeyrie 1965; Van Strydonck and Dupas 1991) and even centuries for voluminous structures (Sonninen et al. 1985). Medieval mortars may still be incompletely carbonated and show an alkaline reaction due to residual $Ca(OH)_2$ (our data). The resolution of the ^{14}C method is a relatively small percentage of the age.

The age, T, of a mortar will be the ages T_n of the n different soluble carbonate phases M_n weighted with their relative proportions, so that:

$$\sum i = 1^n M_i = 1 \tag{3}$$

The apparent age of the whole system, after total dissolution is:

$$T_{tot} = -1/\lambda \ln(M_1 e^{-T1\lambda} + M_2 e^{-T2\lambda} + \ldots M_n e^{-Tn\lambda}) \tag{4}$$

and the age of any single phase is:

$$T_i = -1/\lambda \ln((e^{-Ttot\lambda} - M_1 e^{-T1\lambda} - M_2 e^{-T2\lambda} - \ldots - M_{i-1}e^{-Ti-1\lambda} - M_{i+1}e^{-Ti+1\lambda} - \ldots - M_n e^{-Tn\lambda})/M_i) \tag{5}$$

Incremental dissolution introduces the chemical activities or solubilities of the carbonate phases into the system. The phases M_n will now be split into CO_2 gas for dating and $CaCO_3$ residue. The relation between the gas and the residue is expressed in Equation 2. As the amount of dissolved material from each carbonate phase is a function of time (t), we express the dissolution-time dependent $^{12}C/^{14}C$ ratio accordingly:

$$\frac{N(C12)}{N(C14)} = \frac{M_1^{C12} + M_2^{C12} + \ldots + M_n^{C12} - M_1^{C12}e^{-\Gamma_1 t} - M_2^{C12}e^{-\Gamma_2 t} - \ldots - M_n^{C12}e^{-\Gamma_n t}}{M_1^{C14} + M_2^{C14} + \ldots + M_n^{C14} - M_1^{C14}e^{-\Gamma_1 t} - M_2^{C14}e^{-\Gamma_2 t} - \ldots - M_n^{C14}e^{-\Gamma_n t}} \tag{6}$$

Positive M values represent liberated CO_2 and negative M values represent residual $CaCO_3$. Phases containing only dead carbon can be omitted from the denominator.

MODELING ^{14}C AGE PROFILES

^{14}C profiles from mortar samples are seldom unambiguous, and the correct interpretation of a profile is the key to successful dating. Only rarely do all the dissolution increments yield the same ^{14}C age. The most common and nearly omnipresent contaminant is improperly burned limestone. This is expected since complete calcination (conversion to CaO) is achieved only by maintaining a temperature over 900 °C for hours. This is not worth striving for because the improperly burned residue can just as well comprise part of the filler material. Limestone residues contain, of course, only dead carbon, and they tend to raise the ^{14}C age. However, from experience we know that the residues dissolve relatively slowly in phosphoric acid. A typical profile will therefore start with a rather unaffected mortar binder age, which will be progressively more affected by dead carbon as the dissolution proceeds (Figure 3). Note that we have considered 2 binder phases: one fast and one slow to better mimic a real case. They both have the model age of 700 BP. After about 1 hr of dissolution, the ^{14}C age is strongly affected by the dead carbon.
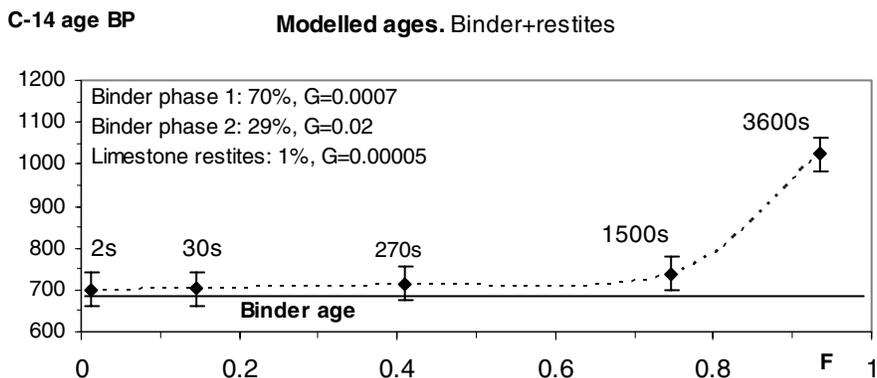

Figure 3 Modeled ^{14}C profile based on 2 binder phases and limestone residues with Γ or G values inserted in the figure. The error bars are set to ±40 yr, a typical value. Dissolution times for the successive increments are also inserted.

Whenever gravel and sand are used as filler in the mortar, it is almost inevitable that there will be some limestone contamination. This is especially the case in limestone areas like the Åland Islands. Figure 4 shows how the profile in Figure 3 is affected by 1% readily-soluble calcite limestone.
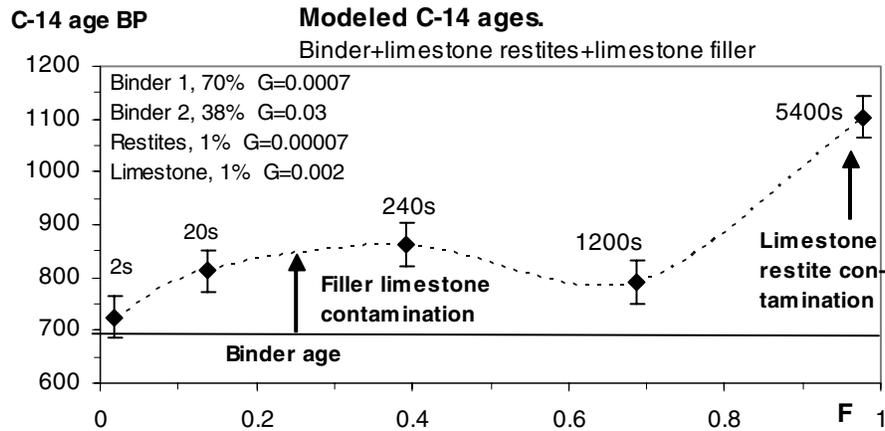
Figure 4 Modeled contamination effects caused by readily-soluble calcitic limestone and slowly dissolving unburned limestone residues. Dissolution constants and time constants are inserted.

Sometimes the mortar is subjected to efflorescent carbonate growth and partial dissolution and recrystallization due to the interaction of acidic waters with alkaline inclusions (e.g. Charola and Lewin 1979; MacLeod et al. 1990). Younger calcites usually dissolve readily and affect only the first dissolution increments. Some examples with non-hydraulic mortars are given later.

MORTARS FROM ÅLAND

Mortar Binders

The binder phase is typically a spongy network of small calcite grains enclosing the aggregate particles. The phase may be micro-crystalline/crypto-crystalline/amorphous. During crystallization, the expelled water (Equation 1) creates porosity and acts as a transporting medium for dissolved CO_2 as CO_3^{2-}. In CL, the binder is usually dark brown with variations from tile red to nearly black. In diagenetic carbonates, there is a relationship between calcite luminescence intensity and pH, Eh, and Mn^{2+} and Fe^{2+} activity in solutions precipitating calcite (Machel 2000). Bright luminescence is promoted by pH-Eh conditions favorable for dissolved Mn^{2+} and precipitation of $Fe(OH)_3$. In most mortars, however, Eh is initially >1 because there is water in contact with atmospheric oxygen, which will lead to precipitation of both Mn and Fe as oxides and hydroxides. Therefore, we do not get the bright luminescence typical of natural calcites. Changing pH conditions during mortar hardening can explain the variety of luminescence intensities of different binder calcite phases in mortars (Figure 5) and among different types of mortars.

In commonly used grain-size fractions spanning from 46–125 µm, our medieval mortars from Åland have yielded about 30% CO_2 as loss on ignition (LOI) (29 ± 3, n = 10) and slightly less during dissolution overnight for dating (25 ± 7). Finer grain-size fractions have higher yields, but we have avoided dating them because they are more difficult to examine microscopically and sometimes they are enriched in small grains from late efflorescent growths. When dating a mortar, the solubility of the binders is monitored prior to CO_2 extraction. Typically, the evolution of CO_2 ceases after about 1 hr at room temperature. Typical values of the dissolution constants (Γ, Equation 2) for the binders at room temperature range from 0.009 to 0.13. Phases with varying solubilities but similar ^{14}C ages coexist. At 0 °C, the reactions are slower and the Γ values smaller. Recently dated samples
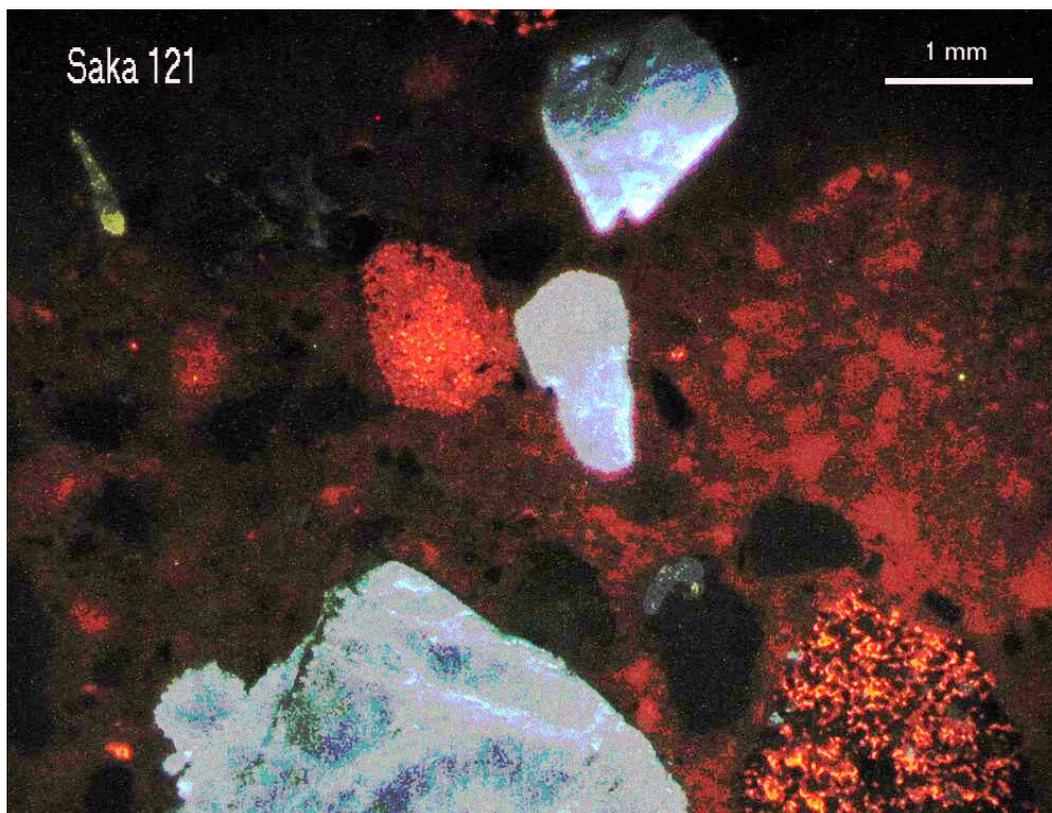
Figure 5 CL micrograph of a sample from the Saltvik church. Tile-red = binder calcite; red-orange = aggregate limestone and calcite matrix in sandstone; blue = quartz; green = feldspar; black = voids, cavities after plucked minerals or non-luminescent minerals. A breccia-like structure is seen in the binder to the right as luminescent early lumps are enclosed in a dull, younger matrix.

from the church of Sund in Åland had Γ values of 0.00063 ± 0.00014 ($n = 6$) at 0 °C, for increments with historically reasonable ^{14}C ages for the 46–75-µm fraction, and F values from 0.3–0.8.

The δ values are determined from the same CO_2 increments as the respective ages. By convention, they denote per mil fractionation versus a standard (e.g. Hoefs 2004). (The standards referred to are indicated in the stable isotope plots.) The $\delta^{13}C$ and $\delta^{18}O$ values for mortars, which yielded the known, expected, or acceptable historical ^{14}C age for more than 50% of the carbonate in the sample, are compiled in Figure 6A–B. Early or late dissolution increments yielding deviating ^{14}C ages are omitted. The $\delta^{13}C$ values have a wide range starting from –22 to –6‰, with an average at 13.1 ± 4.1‰ ($n = 96$). Most of the variation can be explained as kinetic effects controlled by diffusion distance (sampling depth) and the binder/filler ratio (Pachiaudi et al. 1986). $\delta^{18}O$ values are rather low: 11.3 ± 3.2‰ ($n = 70$). They are partly controlled by the delta values for local meteoritic water used in slaking the lime and as an ingredient in the mortar mix. They reflect the high latitude of the Åland Islands, around 60°N, with precipitation of ^{18}O-depleted water (Dansgaard 1964; Yurtsever 1975). Samples with relatively high values around 15‰, e.g. from the church of Sund in Åland (*sund* = strait), may well reflect the presence of brackish water from the Baltic Sea as the church is situated close to a medieval strait (due to postglacial regression it is no longer an open strait).
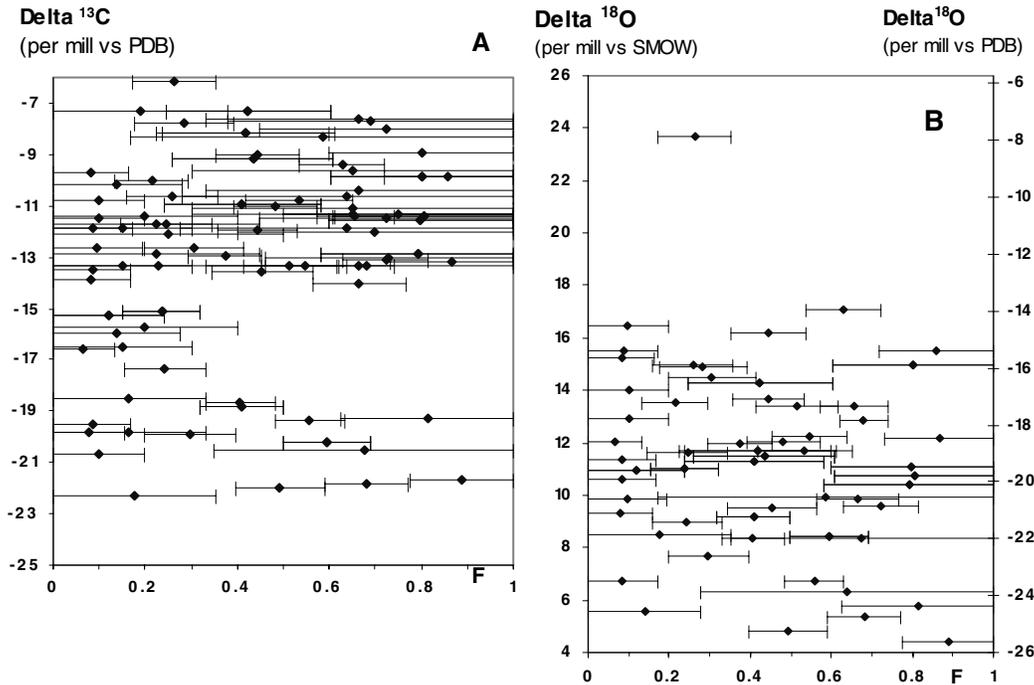
Figure 6 Experimentally determined delta values for calcite binders in non-hydraulic mortars from Åland: A) δ^{13}C (‰ vs Pee Dee Belemnite [PDB]); B) δ^{18}O (‰ vs standard mean ocean water [SMOW] and PDB). The horizontal bars denote the relative increment size and its position ($F_n \rightarrow F_m$) on the abscissa.

Some samples show very little contamination either directly in CL or indirectly in the ^{14}C ages of successive dissolution increments. The stable isotopes for these samples usually display patterns where the δ^{13}C and usually also the δ^{18}O values for the first increments are more negative than the bulk of the mortar. After around 30% dissolution ($F = 0.3$), the δ values reach a maximum, after which they show a decreasing trend. Figure 7 shows the δ^{13}C versus δ^{18}O trend for a sample from a tomb in the church of Sund (Suka 010) and for 1 sample from the nave and another from the sacristy of the Saltvik church (Saka 122 and Saka 148, respectively). In Figure 8, data for the sample from the tomb are presented. (The relation to the chronology of the Sund church is discussed in Ringbom and Remmer [2005]). The dated grain-size fraction contains no luminescent limestone. The last increment was isolated after overnight dissolution at ambient temperature. Although it is so small that there was not enough CO_2 for MS measurements, the last increment is still only slightly affected by unburned limestone residues, and hence the degree of contamination in the other increments is negligible. Due to the careful sample preparation, the whole 46–75-µm grain-size fraction represents only about 1% of the whole sample (The size of the increments and the dissolution times are displayed along the F axis in Figure 8. In some later plots, we will omit these and they will be reported separately in the Appendix).

In Figure 9, two samples from the church of Saltvik are presented. They both display profiles where the contamination effect from the Ordovician limestone (Tynni 1982) is somewhat insignificant. (It is seen as a typical "bump" at the third increment.) In CL, the sample Saka 122 showed 0.20 ± 0.07% luminescent limestone, and in Saka 148, 0.11 ± 0.03% was found. The chronology of the nave versus the sacristy is discussed further in Ringbom and Remmer (2000). The contamination by limestone residues in the final "overnight increments" is also identified on empirical grounds for both
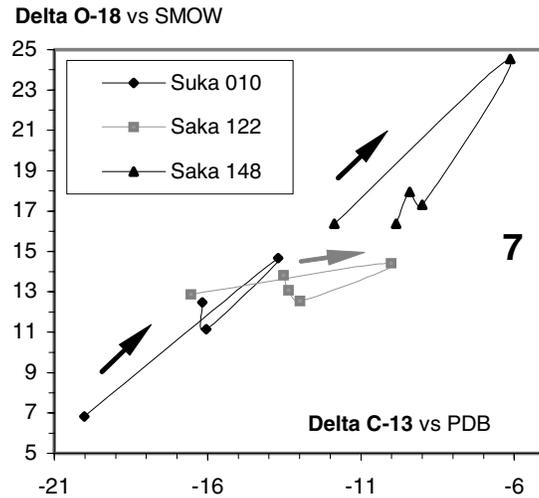
Delta O-18 vs SMOW

Figure 7 $\delta^{13}C$ vs $\delta^{18}O$ for the samples presented in Figures 8 and 9. The arrows indicate trends as functions of increasing *F* values.
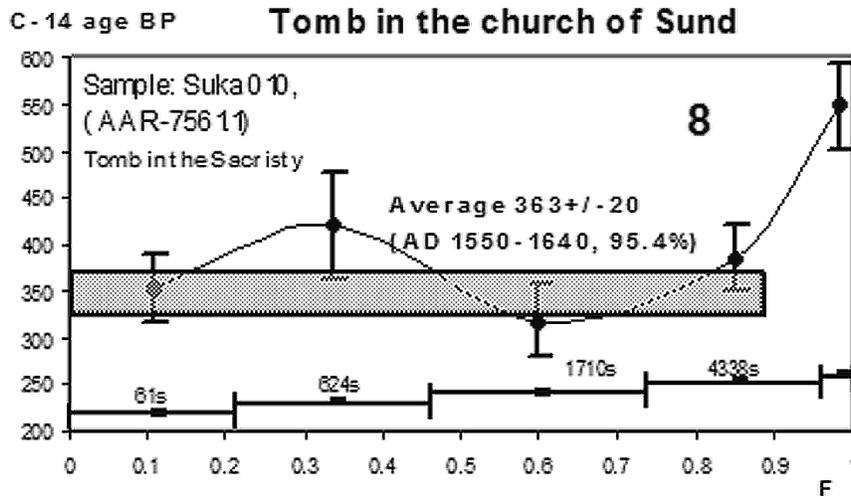

Figure 8 ^{14}C data as a function of dissolution progress for a sample from within the Sund church. The last increment was collected after dissolution overnight.

samples. In Saka 148, the contamination is also statistically significant. In both cases, the increments are rather large and therefore not very sensitive to contamination.

Alkaline and Recrystallized Mortars

Carbonate phases with ^{14}C ages younger than the age of the main binder phase are occasionally found in non-hydraulic mortars (they are common in hydraulic mortars). There appear to be 2 types: calcitic crusts and calcites forming when alkaline inclusions are exposed to CO_2.

Calcitic crusts and stalactite-like formations on the mortar surface and in voids are typical for modern (MacLeod et al. 1990, 1991) and ancient (hydraulic) concrete (Lindroos 2005), but sometimes
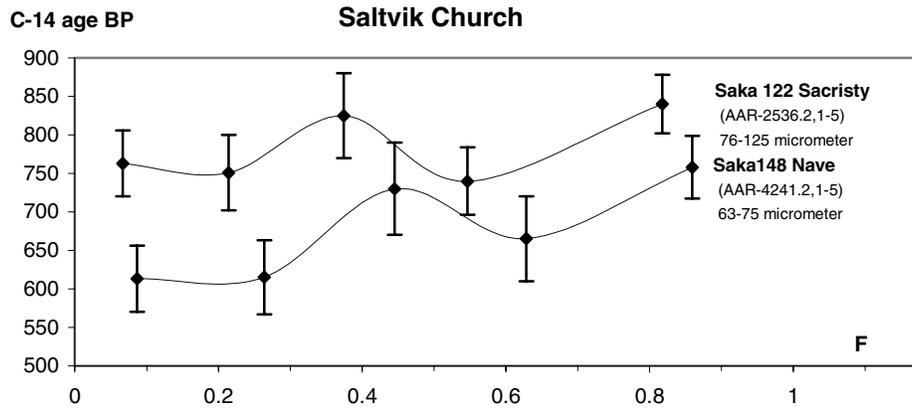
Figure 9 Conventional ^{14}C ages (BP) as a function of the dissolution progress parameter *F*. Each data point is plotted at the middle of the F_n–F_{n+1} interval. The trend lines are only connecting the increments from each sample, and they are not modeled according to the description in the text.

they occur in somewhat non-hydraulic mortars. They form when percolating acidic water comes into contact with alkaline inclusions. Figure 10 shows a piece of mortar where the binder has been partly dissolved and recrystallized calcite has formed a crust around a partly dissolved lime lump. In voids inside the lump, some efflorescent, luminescent crystals have grown. They indicate slower growth in more neutral pH conditions.

Figure 11A shows the ^{14}C age profile of a 5-step incremental dissolution of the same mortar together with the corresponding profile from another similar sample from the same site and chronology. The first increments are affected by the recrystallizations with ^{14}C ages younger than the bulk sample. Figure 11B presents the delta values for the dated increments. Note the low values for both carbon and oxygen for the first increments showing deviating, younger ^{14}C ages. We have not isolated recrystallizations for AMS or MS measurements, but for the first increments there seems to be a relation: the large dissolution relates to constant, young ^{14}C ages and highly negative δ^{13}C values. MacLeod et al. (1990) have measured the stable isotopes in calcite crusts and stalactite-like formations in modern concrete and have found δ^{13}C values from –18.5‰ to –19.2‰ (*n* = 2) corresponding to calcite growth and strong kinetic fractionation in a super-alkaline milieu.

Both of our samples were devoid of luminescent limestone. The age interpretation in Figure 11A, including 7 increments (Suka 017,2–5 and Suka 014,3–5) from these 2 samples, is similar to the age given by Ringbom and Remmer (2005) based on all available data. They suggested an age of AD 1240–1295 for the nave.

Calcites also form when deeper alkaline parts of the mortar are exposed to modern atmospheric CO_2 (or the exhalation of the sampler). The minerals have not been identified directly, but their presence is evident when the mortar shows an alkaline reaction and early dissolution increments show extremely young ^{14}C ages. Table 1 lists the data from a dating of an alkaline sample.

Both types of young calcites seem to be easily soluble and/or concentrated into the most fine-grained grain-size fractions.
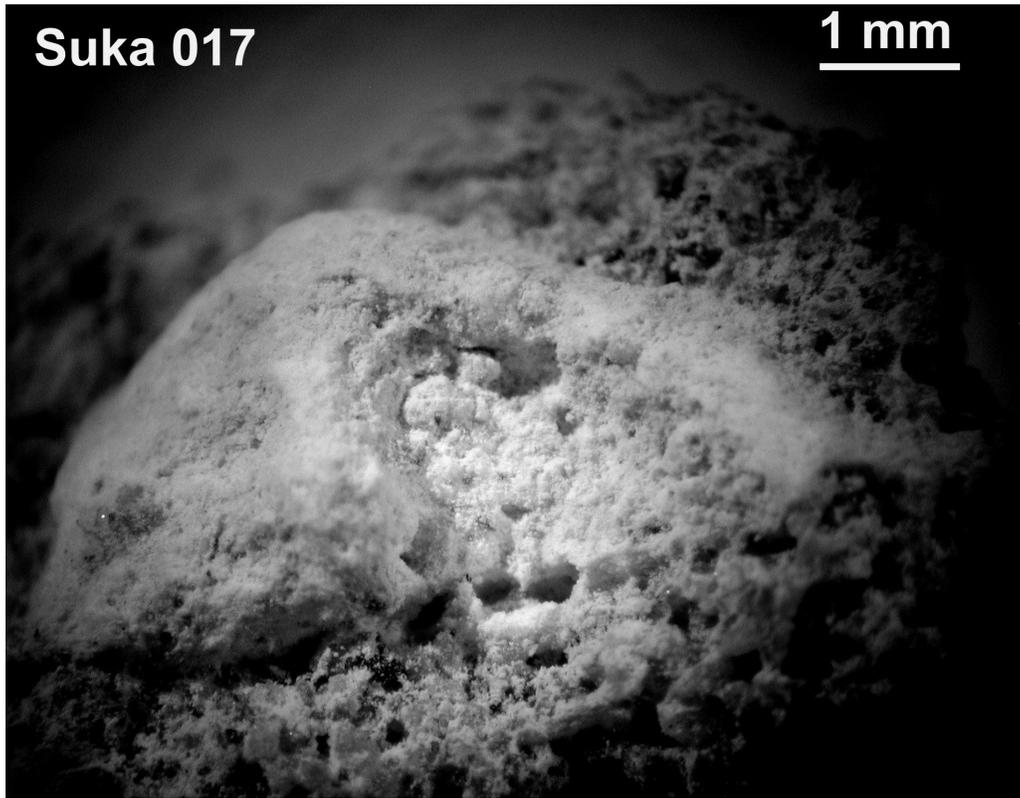
Figure 10 A piece of mortar from the church of Sund (sample Suka 017). Percolating waters have dissolved some of the binder, and new calcites have formed a crust around a lime lump. In voids inside the lump, still younger, light efflorescent calcites have grown.
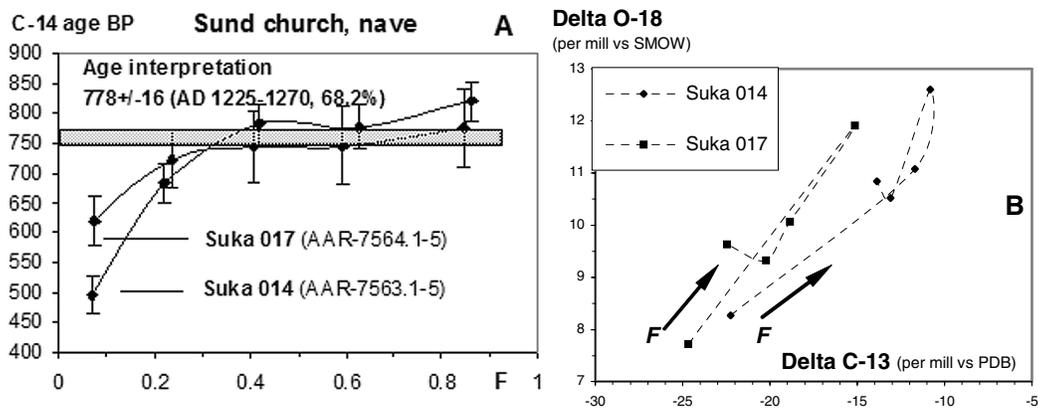
Figure 11 A) ^{14}C age profiles showing the presence of a readily soluble young and minor carbonate phase affecting increment 1 in 2 samples from the same building. B) The contaminated first increments display low delta values.

Table 1 ^{14}C dating result from an alkaline sample (Fika 029a), taken from the sacristy in the church of Finström (δ^{18}O data were not registered when δ^{13}C was measured in 1994).

Sample	*F*	^{14}C age BP	δ^{13}C
AAR-1870,1	0–0.68	–200 ± 60	–14.1
AAR-1870,2	0.69–1	130 ± 80	–14.7

Lime Lumps

White spots or lime lumps can commonly be seen on the surfaces of all kinds of mortar. These spots are the result of poor mixing of lime and aggregate, usually due to lime that has partly hardened already before mixing. Lime lumps may be so abundant that it is impossible to avoid them in sampling for ^{14}C dating. They are also usually softer than the proper binder and yield abundant material to the finest fractions during crushing and sieving. The potential for ^{14}C dating and/or contaminating properties have therefore been tested (Ambers 1987). Actual lime burials have also been dated (Stuiver and Waldren 1975). Van Strydonck et al. (1992) also dated lime lumps from several mortar samples. They found similar age distributions among samples and sample fractions for the lumps as were found for the bulk mortars. The δ^{13}C values were generally higher. We have also done some 2-increment datings of lime lumps and observed similar results (Heinemeier et al. 1997).

We attempted to produce a 5-increment profile for a lime lump from the church in Sund. Because we had a very limited amount of material, we used the larger 76–150-µm grain-size window. The sample showed variable CO_2 yields, and it was difficult to plan the dissolution so that the increments would have similar sizes. Consequently, we ended up with rather irregular increment sizes from 2 separate dissolutions: one with 3 increments and one with only 1 useful increment. The ^{14}C ages of these were compared with the ^{14}C ages from a 4-increment profile of the mortar binder enclosing the lump (Figure 12A). The mortar is very white and full of lumps. It contains about 5% somewhat luminescent carbonates, but a proper segmentation into limestone and luminescent lumps was not possible. The evolution of the delta values during dissolution is presented in Figure 12B.
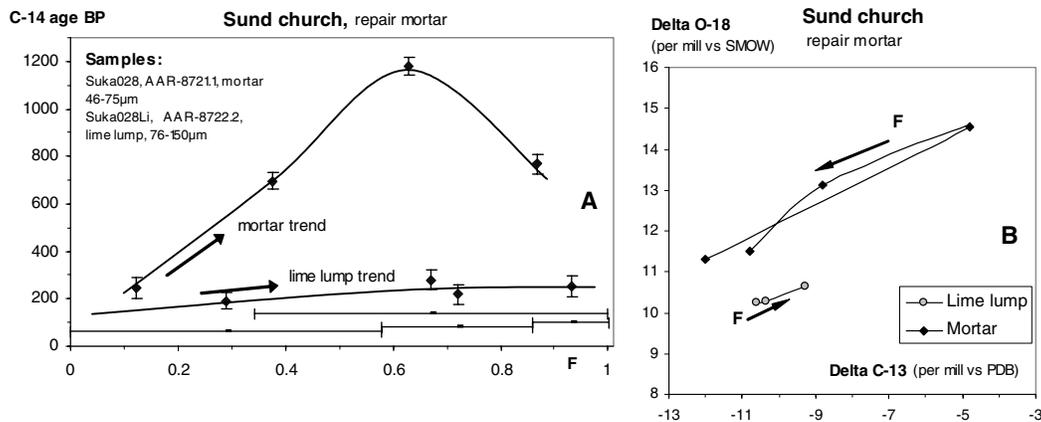
Figure 12 A) ^{14}C age profile for a lime lump compared with corresponding profile for the bulk mortar enclosing the lump. The position and size of the increments are presented with the parameter *F* along the abscissa. The samples are from a repair mortar in the church of Sund, Åland. B) The evolution of the delta values during dissolution (δ^{13}C vs δ^{18}O) for the lump and the binder, respectively. Note that the first CO_2 increment from the bulk mortar was actually lost and no MS data is available. The δ^{13}C value (–12) is a measurement from the tandem accelerator and the δ^{18}O value is set to 13, a local average.

The increments from the lime lump show rather uniform ^{14}C ages and delta values. The dissolution constant attained the values 0.0001–0.0002 at 0 °C. Unfortunately, these values are not very useful because of the large grain-size window and the unpredictable dissolution behavior. The lime lumps, however, seem to be composed of 1 calcite phase with 1 ^{14}C age or a narrow distribution of ages, which can be connected to the building or repair history. The spans in delta values reflect only kinetic fractionation during dissolution (note that the incremental dissolution displays differences between early increments and residues more efficiently than a cumulative procedure). The binder, on the other hand, is severely contaminated by local Ordovician limestone, and the ^{14}C ages are of little use in archaeometry. A preliminary conclusion is that lime lumps are not contaminants from an archaeometric point of view, but are a datable component. It is, however, important to identify them and distinguish them from limestone residues.

Aggregate Limestone

A non-hydraulic lime-mortar paste usually includes an aggregate of sedimentologic origin, such as beach sand and gravel or corresponding fluvial material. In the Åland Islands, there is a basement composed of granite and an overburden composed of granite sand and gravel and limestone originating from the bottom of the Baltic Sea. In general, the filler materials contain some calcite, and the calcite will contribute its geological age to the dating. There may also be other carbonates, but they are either poorly soluble (e.g. dolomite, magnesite, ankerite) or unstable and/or rare (e.g. aragonite, vaterite, strontianite). Consequently, we must ask how much geological calcite there is and how it dissolves. The mortar samples can be examined petrographically from uncovered thin sections using a petrographic microscope and CL. This reveals which carbonates are present and what they look like. Semi-quantitative assessments of the amount of geological carbonate can be made using point counting or image analysis of CL micrographs of sieved grain-size fractions for dating. There are, however, many problems involved in this approach (Lindroos 2005). In our experience, the worst problem is the identification of geological calcites lacking luminescence. Figure 13A shows an example where soft, devitrified limestone with very weak luminescence contaminated the fine fractions in a sample series from the Vårdö church.

The chemical activity of the limestone contaminating the samples can be deduced from Figure 13A. The ^{12}C/^{14}C ratio is at its maximum after about 40% dissolution ($F = 0.4$). This means that the limestone dissolves slower than part of the mortar. Note, however, that the maxima in delta values occur in the second increments (Figure 13B) and the ^{14}C age maxima occur in the third increments. This is typical for samples from Åland. Lime lump material with high delta values is far more common in fine fractions than limestone splinter, yet these may have similar delta values. The lumps have the maximum relative activity at about 30% dissolution and the Ordovician limestone a little later. It is obvious that the delta values are poor parameters for monitoring contaminating effects. Any variation in delta values due to limestone contamination is effectively masked by a broad spectrum of values for the proper binder and the high values for the lumps.

Interference of Several Contaminants

In this section, we will describe some typical cases where the features described above are either easy to identify or they interfere so that it might be difficult to interpret the ^{14}C profiles for archaeometry. The nave of the Hammarland church was dated in 1994 and 1995; the results are published in Ringbom and Remmer (1995). The samples represent a rather heterogeneous data set. Seventeen samples were dated in 2 CO_2 fractions. After considering different clusters of data, 4 different alternatives were presented: 715 ± 25 BP, 690 ± 15 BP, 675 ± 20 BP, and 650 ± 20 BP. A more homogenous data set for the tower of the church yielded a similar age distribution, although the tower is
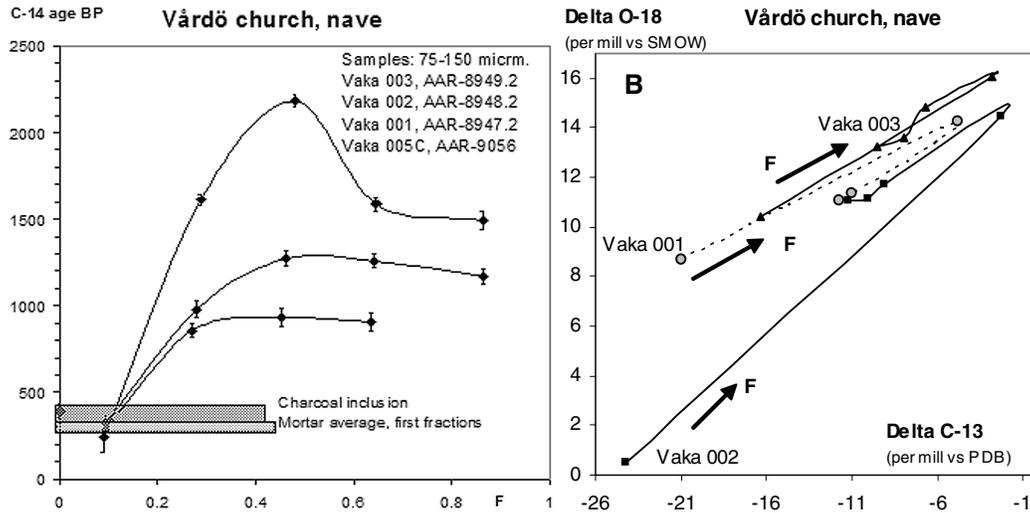
Figure 13 A) ^{14}C age profiles for 3 mortar samples contaminated with devitrified Ordovician limestone. The age of a charcoal inclusion (the horizontal line) defines a maximum age. B) Stable isotope patterns for the same samples. Extremely low delta values for 2 early CO_2 increments indicate the presence of recrystallizations.

clearly secondary in relation to the nave. The average of 3 samples (6 CO_2 fractions) is 690 ± 25 BP, and the average of the first fractions only is 685 ± 35 BP. Two samples were re-dated as a control in 5-increment profiles 2004 (Figure 14). Sample Haka 052 has 0.22 ± 0.16% luminescent limestone, while Haka 055 has 0.14 ± 0.07%, but part of the limestone is dolomitic. The profiles suggest that there are mortars from the second half of the 13th century in the nave, and the nave seems to be a few decades older than the tower. Four charcoal inclusions from other mortar samples from the nave are clearly older (Figure 14). These 2 samples show typical contamination patterns similar to the model in Figure 4. The mid-parts of the profiles are contaminated by filler limestone, and there are typical effects from poorly calcinated limestone residues in the last increments. If we model the contamination, the same Γ values can be used for both samples.

In Saltvik, dendrochronological analyses from 9 pine logs suggest a building phase in the second half of the 14th century, probably in the early 1370s (Ringbom and Remmer 2000). In the late 1990s, we performed mortar datings on a number of samples. The average age for the first fractions ($n = 10$) was 643 ± 11 BP. This age was used for archaeometry. Due to the nature of the calibration curve at this point, the resolution is very poor, but it corresponds to the 14th century. Two samples were reanalyzed as ^{14}C profiles. The sample Saka 146 is contaminated with 0.14 ± 0.08% and Saka 148 with 0.11 ± 0.03% luminescent limestone according to our IA assessments. Figure 15 shows the results. The profiles yield the same age as earlier and they verify that it was a correct approach to utilize the first fractions for archaeometry. Note, however, how important it is to use several samples. Taken alone, the profile from sample Saka 146 could be misinterpreted to suggest an age where the profile levels out at about 900 BP.

The mortar from the nave of the church of Eckerö has been dated by Ringbom and Remmer (1995; in 2 CO_2 fractions only) and re-dated by Ringbom et al. (2006). The first fractions of 8 samples yielded the average age 718 ± 25 BP, corresponding to AD 1270–1290 (68.2% confidence level). One sample was re-dated as a profile 2004 (Figure 16). In CL, this sample seems contaminated: 0.39 ± 0.15% limestone was assessed and 1.71 ± 0.41% somewhat luminescent limestone residues
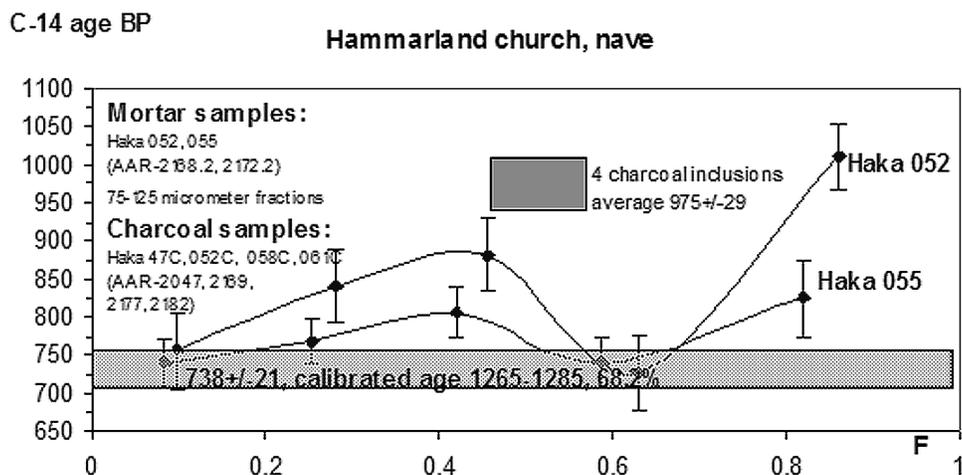
C-14 age BP

Hammarland church, nave

Figure 14 ^{14}C profiles for 2 mortar samples from the nave in the church of Hammarland. The average age of 4 charcoal inclusions is included.
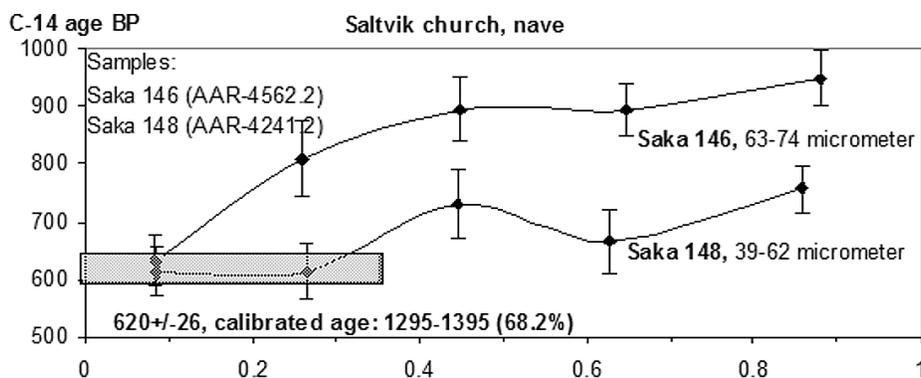

Figure 15 ^{14}C profiles for 2 mortar samples from the nave of the church in Saltvik. The mortar age 620 ± 26 has been calculated from the 3 CO_2 fractions within the gray field. Other fractions are considered contaminated by filler limestone and unburned limestone as described above.

were also identified. The results are presented together with the older data for the same sample. The 6 fractions with the youngest ages define a cluster with the combined age of 720 ± 25 BP. A chip of wood in the sample turned out to be about 100 yr older than the mortar.

CONCLUSIONS

Mortars are heterogeneous carbonate systems and dating them using ^{14}C requires detailed studies of the carbonates and, in particular, their solubilities. Ideally, a series of samples from each mortar batch should be analyzed. In the 1990s, we dated mortar in masonry constructions using an AMS modification of the "Texas method": the mortars were allowed to react with phosphoric acid for only a few seconds, and the dating was conducted on the CO_2 that was initially liberated. The residue of the sample was dated for reference and contamination control only. The results from the first CO_2 fractions were treated statistically considering the averages from age clusters and rejecting outliers. In the late 1990s, cathodoluminescence (CL) control was introduced, and in many cases samples could be rejected already before AMS analysis, which resulted in cost savings and more coherent
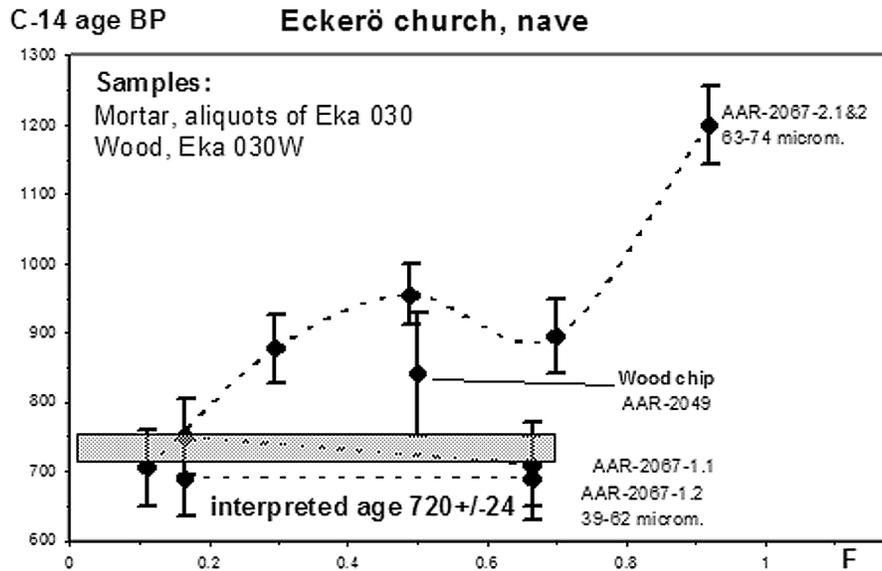
Figure 16 ^{14}C profile including 5 CO$_2$ fractions presented together with older data from the same sample (in 2 fractions).

age clusters for the mortar batches, respectively. After some trials with hydraulic mortars including readily soluble recrystallizations, we modified the dating procedure so that each sample is now dated in 5 or more fractions representing successive CO$_2$ increments from a dissolution procedure lasting up to 18 hr. Each sample is thereby described in terms of ^{14}C age and δ^{13}C-δ^{18}O profiles plotted versus the dissolution progress variable *F*. The introduction of the profiles has helped us to understand and even model some of the contamination effects commonly encountered in the dating. We have also become more aware of the risk connected with readily soluble recrystallizations, which sometimes contaminate the first fractions of non-hydraulic, as well as hydraulic, mortars. Our experience from the mortars from the Åland Islands has been most useful for our work on the development of the method for a more general use, including hydraulic mortars in samples from classical and medieval Rome, and we are now concentrating on defining the limits of the implementation of mortar dating. After dating some 250 samples from Åland, Norway, Portugal, Spain, and Italy, we can conclude that the least problematic samples have been clearly non-hydraulic mortars without ashes from areas with crystalline basement rocks. In favorable cases, when the mortar is clearly non-hydraulic, the filler material has very few carbonates (which are preferably dolomitic marble), and the site has an arid climate. It may be possible to reduce the number of CO$_2$ fractions from each sample. However, our work in the Åland Archipelago shows that even if the local soils and mortar fillers may have abundant limestone, dating is still possible. Although mortar dating is a rather expensive method, sometimes mortar is the only datable material available and often mortar dating is an alternative to even more expensive, large-scale excavations.

ACKNOWLEDGMENTS

REFERENCES

Ambers J. 1987. Stable carbon isotope ratios and their relevance to the determination of accurate radiocarbon dates for lime mortars. *Journal of Archaeological Science* 14:569–76.

Baxter MS, Walton A. 1970. Radiocarbon dating of mortars. *Nature* 225(5236):937–8.

Charola AE, Lewin SZ. 1979. Efflorescences on building stones. SEM in the characterization and elucidation of the mechanisms of formation. *Scanning Electron Microscopy* 1:379–86.

Dansgaard W. 1964. Stable isotopes in precipitation. *Tellus* 16:436–68.

Deer WA, Howie RA, Zussman J. 1992. *An Introduction to the Rock-Forming Minerals.* 2nd edition. New York: Wiley. 696 p.

Delibrias G, Labeyrie J. 1965. The dating of mortars by the carbon-14 method. In: Chatters RM, Olson EA, editors. Proceedings from the 6th International Conference on ^{14}C and Tritium Dating. Washington, D.C.: Clearinghouse for Federal Scientific & Technological Information, Natural Bureau of Standards. U.S. Dept. Commerce. p 344–7.

Folk RL, Valastro S Jr. 1976. Successful technique for dating of lime mortars by carbon-14. *Journal of Field Archaeology* 3:203–8.

Habermann D, Neuser RD, Richter K. 2000. Quantitative high resolution spectral analysis of Mn^{2+} in sedimentary calcite. In: Pagel M, Barbin V, Blanc P, Ohnenstetter D, editors. *Cathodoluminescence in Geosciences.* New York: Springer-Verlag. p 331–58.

Hale J, Heinemeier J, Lancaster L, Lindroos A, Ringbom Å. 2003. Dating ancient mortar. *American Scientist* 91(2):130–7.

Heinemeier J, Jungner H, Lindroos A, Ringbom Å, von Konow T, Rud N. 1997. AMS ^{14}C dating of lime mortar. *Nuclear Instruments and Methods in Physics Research B* 123(1–4):487–95.

Hoefs J. 2004. *Stable Isotope Geochemistry.* 5th edition. New York: Springer-Verlag. 244 p.

Labeyrie J, Delibrias G. 1964. Dating of old mortars by the carbon-14 method. *Nature* 201(4920):742.

Lindroos A. 2005. Carbonate phases in historical building mortars and pozzolana concrete. Implications for AMS ^{14}C dating [FD thesis]. Turku, Finland: Åbo Akademi University. ISBN 952-12-1560-7. 92 p.

Machel H. 2000. Application of cathodoluminescence to carbonate diagenesis. In: Pagel M, Barbin V, Blanc P, Ohnenstetter D, editors. *Cathodoluminescence in Geosciences.* New York: Springer-Verlag. p 271–301.

MacLeod G, Hall AJ, Fallick AE. 1990. An applied mineralogical investigation of concrete degradation in a major concrete road bridge. *Mineralogical Magazine* 54:637–44.

MacLeod G, Hall AJ, Fallick AE. 1991. Mechanism of carbonate mineral growth on concrete structures as elucidated by carbon and oxygen isotope analyses. *Chemical Geology* 86:335–43.

Marshall DJ. 1988. *Cathodoluminescence of Geological Materials.* Boston: Unwin Hyman. 146 p.

Pachiaudi C, Marechal J, Van Strydonck M, Dupas M, Dauchot-Dehon M. 1986. Isotopic fractionation of carbon during CO_2 absorption by mortar. *Radiocarbon* 28(2A):691–7.

Ringbom Å, Remmer C. 1995. *Ålands Kyrkor. Volume I. Hammarland Och Eckerö.* Ålands landskapsstyrelse/museibyrån. 300 p. In Swedish with English summary.

Ringbom Å, Remmer C. 2000. *Ålands Kyrkor. Volume II. Saltvik.* Ålands landskapsstyrelse/museibyrån. 300 p. In Swedish with English summary.

Ringbom Å, Remmer C. 2005. *Ålands Kyrkor. Volume III. Sund Och Vårdö.* Ålands landskapsstyrelse/museibyrån. 336 p. In Swedish with English summary.

Ringbom Å, Lindroos A, Heinemeier J, Lancaster L, Hale J. 2003. When did mortar harden? [abstract]. XVI International Congress of Classical Archaeology, AIAC conference. 23–26 August 2003, Cambridge, Massachusetts, USA. Harvard University. p 54–5.

Ringbom Å, Hale J, Heinemeier J, Lindroos A, Brock F. 2006. Mortar dating in medieval and classical archaeology. *Construction History Newsletter* 73:10–7.

Sonninen E, Erämetsä P, Jungner H. 1985. Dating of mortar and bricks from the castle of Kastelholm. *Iskos* 5:384–9.

Stuiver M, Smith CS. 1965. Radiocarbon dating of ancient mortar and plaster. In: Chatters RM, Olson EA, editors. Proceedings of the 6th International Conference on Radiocarbon and Tritium Dating. Washington, D.C.: Clearinghouse for Federal Scientific & Technological Information, Natural Bureau of Standards. U.S. Department of Commerce. p 338–43.

Stuiver M, Waldren WH. 1975. ^{14}C carbonate dating and the age of post-Talayotic lime burials in Mallorca. *Nature* 255(5508):475–6.

Swart PK, Burns SJ, Leder JJ. 1991. Fractionation of the stable isotopes of oxygen and carbon in carbon dioxide during the reaction of calcite with phosphoric acid as a function of temperature and technique. *Chemical Geology* (Isotope Geoscience Section) 86:89–96.

Tynni R. 1982. On Paleozoic microfossils in clastic dykes on the Åland Islands and in the core samples from Lumparn. In: Paleozoic Sediments in the Rapakivi Area of the Åland Islands. *Geological Survey of Finland, Bulletin* 317:35–94.

Van Strydonck M, Dupas M. 1991. The classification and dating of lime mortars by chemical analysis and radiocarbon dating: a review. In: Waldren WH, Ensenyat JA, Kennard RC, editors. Second Deya International Conference of Prehistory. Volume II. *BAR International Series* 574:5–43

Van Strydonck M, Dupas M, Dauchot-Dehon M. 1983. Radiocarbon dating of old mortars. In: Mook WG, Waterbolk HT, editors. ^{14}C and Archaeology, Pro-

ceedings. *PACT* 8:337–43.

Van Strydonck M, Dupas M, Dauchot-Dehon M, Pachiaudi C, Marechal J. 1986. The influence of contaminating (fossil) carbonate and the variation of δ¹³C in mortar dating. *Radiocarbon* 28(2A):702–10.

Van Strydonck M, Dupas M, Keppens E. 1989. Isotopic fractionation of oxygen and carbon in lime mortar under natural environmental conditions. *Radiocarbon* 31(3):610–8.

Van Strydonck MJY, van der Borg K, de Jong AFM, Keppens E. 1992. Radiocarbon dating of lime fractions and organic material from buildings. *Radiocarbon* 34(3):873–9.

Wachter EA, Hayes JM. 1985. Exchange of oxygen isotopes in carbon dioxide-phosporic acid systems.

Chemical Geology (Isotope Geoscience Section) 52: 365–74.

Walters LJ, Claypool GE, Choquette PW. 1972. Reaction rates and δ¹⁸O variation for the carbonate-phosphoric acid preparation method. *Geochimica et Cosmochimica Acta* 36(2):129–40.

Willaime B, Coppens R, Jaegy R. 1983. Datation des mortiers du château de Châtel-sur-Moselle per le carbon 14. In: Mook WG, Waterbolk HT, editors. ¹⁴C and Archaeology, Proceedings. *PACT* 8:345–50. In French.

Yurtsever Y. 1975. Worldwide survey of stable isotopes in precipitation. Rep. Isotope Hydrology Section. November 1975. Vienna: IAEA. 40 p.

APPENDIX

Dated samples and sample fractions (in order in which they occur in the text).

Sample	Lab nr Århus (AAR-)	Locality	Carbon yield (%) and grain-size fraction (μm)	Fraction size (%) per dissolution time	¹⁴C age (BP)	δ¹³C ‰ vs PDB	δ¹⁸O ‰ vs PDB (85% H_3PO_4)
Suka 034	7570,1	Sund church, sacristy	4.6; 46–75	16.9 per 71 s	451 ± 43	−13.50	−18.11
	7570,2			27.7 per 5.2 min	743 ± 43	−8.06	−15.49
	7570,3			23.1 per 22.9 min	728 ± 39	−10.11	−17.36
	7570,4			20.6 per 80.5 min	835 ± 33	−10.74	−16.25
	7570,5			11.7 per 16 hr	1275 ± 38	−10.78	−16.14
Suka 010	7561,1	Sund church, tomb	3.0; 46–75	21.3 per 61 s	354 ± 36	−20.03	−23.30
	7561,2			25.0 per 10.4 min	420 ± 55	−13.07	−15.69
	7561,3			27.3 per 28.5 min	318 ± 39	−16.04	−19.11
	7561,4			22.6 per 72.3 min	385 ± 37	−16.17	−17.83
	7561,5			3.8 per 16 hr	548 ± 45	−17 (AMS)	
Saka 122	2537-2,1	Saltvik church, sacristy	7.9; 76–125	13.3 per 90 s	763 ± 42	−16.55	−17.45
	2537-2,2			16.2 per 8.2 min	751 ± 50	−10.02	15.95
	2537-2,3			15.9 per 21.5 min	825 ± 55	−12.98	−17.48
	2537-2,4			32.7 per 32.7 min	740 ± 55	−13.36	−17.26
	2537-2,5			36.5 per 16 hr	840 ± 55	−13.53	−16.52
Saka 148	4241-2,1	Saltvik church, nave	6.6; 39–62	17.3 per 61 s	613 ± 43	−11.87	−14.05
	4241-2,2			18.1 per 3.3 min	615 ± 48	−6.13	−6.13
	4241-2,3			18.2 per 14.7 min	730 ± 60	−9.00	−13.14
	4241-2,4			18.5 per 21.5 min	665 ± 55	−9.41	−12.52
	4241-2,5			28.2 per 16 hr	758 ± 41	−9.86	−14.04
Suka 014	7563,1	Sund church, nave	5.9; 46–75	14.4 per 16 s	496 ± 32	−22.26	−21.96
	7563,2			15.7 per 49 s	683 ± 33	−11.9	−19.74
	7563,3			23.3 per 7 min	781 ± 33	−10.81	−17.76
	7563,4			18.8 per 13 min	777 ± 36	−13.09	−19.78
	7563,5			27.8 per 16 hr	819 ± 33	−13.87	−19.47

Dated samples and sample fractions (in order in which they occur in the text). *(Continued)*

Sample	Lab nr Århus (AAR-)	Locality	Carbon yield (%) and grain-size fraction (μm)	Fraction size (%) per dissolution time	^{14}C age (BP)	$\delta^{13}C$ ‰ vs PDB	$\delta^{18}O$ ‰ vs PDB (85% H_3PO_4)
Suka 017	7564,1	Sund church,	5.9; 46–75	15.2 per 38 s	619 ± 42	–24.69	–22.49
	7564,2	nave		16.6 per 52 s	723 ± 49	–15.13	–18.43
	7564,3			18.1 per 10.1 min	745 ± 60	–18.84	–20.22
	7564,4			19.1 per 22.8 min	745 ± 65	–20.22	–20.94
	7564,5			31.1 per 16 hr	775 ± 65	–22.47	–20.64
Suka 028	8721,1	Sund church,	3.0; 46–75	24.6 per 27 s	246 ± 43	–12 (AMS)	
	8721,2	nave attic		26.2 per 66 s	697 ± 34	–4.80	–15.84
	8721,3			24.2 per 6.9 min	1182 ± 38	–8.81	–17.12
	8721,4			23.4 per 23.9 min	768 ± 41	–10.79	–18.77
	8721,5			1.6 per 16 hr	(lost)	—	—
Suka 028 Li Lime lump	8722-2,1	Sund church,	11.1; 75–150	57.8 per 51 min	192 ± 35	–10.61	–20.01
	8722-2,2	nave attic		28.3 per 103.6 min	219 ± 40	–10.34	–19.95
	8722-2,3			14.1 per 16 hr	253 ± 43	–9.28	–19.61
	8722-2,5,1			65.9 per 16 hr	279 ± 40	–10.26	–21.26
Vaka 001	8947-2,1	Vårdö church,	4.9; 76–150	18.5 per 30 s	287 ± 36	–21.01	–21.56
	8947-2,2	gable of the		17.1 per 6.9 min	857 ± 40	–4.79	–16.16
	8947-2,3	chancel		19.4 per 19.4 min	933 ± 50	–11.06	–19.00
	8947-2,4			17.1 per 45 min	905 ± 55	–11.78	–19.36
Vaka 002	8948-2,1	Vårdö church,	5.0; 76–150	18.9 per 27 s	319 ± 43	–24.23	–29.52
	8948-2,2	gable of the		18.2 per 2.9 min	979 ± 45	–2.35	–15.98
	8948-2,3	chancel		18.2 per 14.7 min	1274 ± 47	–9.12	–18.65
	8948-2,4			17.9 per 24.5 min	1258 ± 42	–10.09	–19.15
	8948-2,5			27.2 per 16 hr	1167 ± 44	–11.25	–19.26
Vaka 003	8948-2,1	Vådrö church,	3.8; 76–150	18.0 per 46 s	240 ± 90	–16.36	–19.19
	8948-2,2	gable of the		21.4 per 5.6 min	1611 ± 32	–2.88	–14.14
	8948-2,3	chancel		17.0 per 19.9 min	2181 ± 36	–6.71	–15.60
	8948-2,4			16.5 per 42.3 min	1586 ± 36	–8.02	–16.80
	8948-2,5			27.5 per 16 hr	1495 ± 55	–9.58	–17.13
Vaka005C charcoal	9056	Vårdö church, gable of the chancel			394 ± 41	–26.04	
Saka 146	4562-2,1	Saltvik church,	6.1; 63–74	16.5 per 150 s	632 ± 44	–9.69	–14.36
	4562-2,2	nave		19.0 per 13.8 min	810 ± 65	–7.46	–13.38
	4562-2,3			18.7 per 24.0 min	895 ± 55	–9.15	–15.08
	4562-2,4			20.8 per 43.6 min	894 ± 46	–9.46	–15.09
	4562-2,5			24.2 per 16 hr	948 ± 48	–9.20	–14.71
Saka 148	4241-2,1	Saltvik church,	6.6; 39–62	17.3 per 61 s	613 ± 43	–11.87	–14.05
	4241-2,2	nave		18.1 per 3.3 min	615 ± 48	–6.13	–6.13
	4241-2,3			18.2 per 14.7 min	730 ± 60	–9.00	–13.14
	4241-2,4			18.5 per 21.5 min	665 ± 55	–9.41	–12.52
	4241-2,5			28.2 per 16 hr	758 ± 41	–9.86	–14.04

Dated samples and sample fractions (in order in which they occur in the text). *(Continued)*

Sample	Lab nr Århus (AAR-)	Locality	Carbon yield (%) and grain-size fraction (μm)	Fraction size (%) per dissolution time	^{14}C age (BP)	δ^{13}C ‰ vs PDB	δ^{18}O ‰ vs PDB (85% H$_3$PO$_4$)
Haka 052	3168-2,1	Hammarland church, nave	2.9; 76–125	19.5 per 45 s	756 ± 44	–17.04	–13.53
	3168-2,2			17.1 per 2.6 min	841 ± 43	–3.98	–16.19
	3168-2,3			18.1 per 12.5 min	882 ± 44	–9.19	–18.52
	3168-2,4			16.9 per 27.3 min	729 ± 33	–9.72	–19.12
	3168-2,5			28.1 per 16 hr	1010 ± 55	–11.04	–19.07
Haka 055	2172-2,1	Hammarland church, nave (partially lost)	3.0; 76–125	16.8 per 127 s	739 ± 32	–13.85	–18.83
	2172-2,2			17.0 per 8.7 min	768 ± 30	–8 (AMS)	
	2172-2,3			16.4 per 19.6 min	807 ± 33	–10.25	–18.60
	2172-2,4			17.1 per 34.1	740 ± 33	–8.68	–14.32
	2172-2,5			32.0 per 16 hr	825 ± 50	–10.32	–19.28
Eka 030	2067-2.2,1	Eckerö church, nave	7.7; 63–74	22.1 per 84 s	705 ± 55	–19.64	–19.94
	2067-2.2,2			27.0 per 8.5 min	(lost)	—	—
	2067-2.2,3			23.9 per 16.9 min	955 ± 44	–14.62	–17.89
	2067-2.2,4			17.9 per 77.7 min	895 ± 55	–15.42	–17.39
	2067-2.2,5			8.7 per 16 hr	1200 ± 50	–15 (AMS)	
	2067-2.1,1	(aliquot)	7.7; 63–74	14.9 per 36 s	(lost)	—	—
	2067-2.1,2			17.3 per 102 s	889 ± 49	–7.73	–14.94